Science in China Series D: Earth Sciences

SCIENCE IN CHINA PRESS

Springer

Three-dimensional thermal structure of the Chinese continental crust and upper mantle

AN MeiJian[1,2†] & SHI YaoLin[1]

[1] Laboratory of Computational Geodynamics, Graduate University of Chinese Academy of Sciences, Beijing 100049, China;
[2] Key Laboratory of Crust Deformation and Processes and Institute of Geomechanics, Chinese Academy of Geological Sciences, Beijing 100081, China

We invert S-wave velocities for the 3D upper-mantle temperatures, in which the position with a temperature crossing the 1300℃ adiabat is corresponding to the top of the seismic low velocity zone. The temperatures down to the depth of 80 km are then calculated by solving steady-state thermal conduction equation with the constraints of the inverted upper-mantle temperatures and the surface temperatures, and then surface heat flows are calculated from the crustal temperatures. The misfit between the calculated and observed surface heat flow is smaller than 20% for most regions. The result shows that, at a depth of 25 km, the crustal temperature of eastern China (500—600℃) is higher than that of western China (<500℃). At a depth of 100 km, temperatures beneath eastern and southeastern China are higher than the adiabatic temperature of 1300℃, while that beneath west China is lower. The Tarim craton and the Sichuan basin show generally low temperature. At a depth of 150 km, temperatures beneath south China, eastern Yangtze craton, North China craton and around the Qiangtang terrane are higher than the adiabatic temperature of 1300℃, but is the lowest beneath the Sichuan basin and the regions near the Indian-Eurasian collision zone. At a depth of 200 km, very low temperature occurs beneath the Qinghai-Tibet Plateau and the south to the Tarim craton.

crust, upper mantle, temperature, seismic velocity, China

1 Introduction

Temperature is one of the most important geophysical quantities. For example, temperature gradient in the mantle controls mantle convection, which in turn drives plate tectonics and earthquake occurrences. In addition, many geologic processes such as some of ore formation are directly related to thermal anomalies.

Some of thermal properties of the Earth can be measured directly from the surface, such as surface temperature gradient, heat productivity and conductivity of rocks. The crustal and upper-mantle heat productivities are often estimated from seismic velocities using some relationship obtained from the laboratory tests of rock samples[1]. Using surface heat flow observation as a boundary condition, one can construct the thermal structure of the lithosphere by solving the steady-state thermal conduction equation[2−5]. With this method, Artemieva and Mooney[1] estimated lithosphere temperatures of the Precambrian regions in the world; Wang[3] calculated lithospheric temperatures for some regions of China.

The above traditional temperature calculation method has obvious disadvantages. First, the thermal measurements made on the Earth's surface are often influenced by recent/ancient tectonics and environment, e.g., denudation, sedimentation and subterranean water. Due to the scarcity of information on these factors, the heat flow data, even after correction, often contain uncertainties up

Received November 6, 2006; accepted March 19, 2007
doi: 10.1007/s11430-007-0071-3
†Corresponding author (email: meijianan@yahoo.com.cn)
Supported by China Postdoctoral Science Foundation, Key Program of NSFC (National Science Foundation of China) (Grant No. 40234042), and NSFC (Grant Nos. 40674058 and 40374038)

to ~20%[6]. Besides, the conductivity and heat productivity of deep rocks are chosen with uncertainties which may cause considerable uncertainties in the calculated temperature. For instance, a 5% change in heat flow may cause a temperature change of 50－90℃ at 100 km depth; a 20% change in heat productivity may cause 100－130℃ of temperature change at 100 km depth[1]. Such uncertainties are expected to increase with increasing depth.

It is notable that, the above studies based on the assumption that the lithosphere has been stable for a long time (>500 Ma)[7]. But such assumption often may not be satisfied, especially in tectonically active regions. In the Chinese continent, the crusts of the North China, Yangtze and Tarim cratons are very old, but their surfaces have suffered various modifications during the long geological period, mainly due to the tectonic interaction between neighboring blocks and the thermal actions at/below the base of the lithosphere. It is well accepted that the ancient North China and Yangtze cratons were strongly reshaped by Phanerozoic tectonic events[8]. Although crustal evidence shows that Phanerozoic reworking of the Tarim craton is relatively weak, the mantle may be strong. For example, the thermal lithosphere, estimated based on a steady-state assumption[1,9] and measured surface heat flow, is far thicker (by ~100 km) than the seismological lithosphere and the seismic-thermal lithosphere[10]. So, it is difficult to find a region in the Chinese continent that satisfies the steady-state assumption.

Seismic velocities of deep lithosphere were related to surface heat flow[11], but apparently to deep thermal structure[12,13]. On the basis of many studies and experiments, Goes et al.[14] proposed a seismic-thermal method to calculate upper mantle temperatures from seismic velocities. This method was applied in the European and North American continents[14－17].

In this method, elastic-wave velocities are calculated from elastic parameters and density and their variations with temperature, pressure and compositions on the basis of laboratory tests. But our objective is to determine temperatures and compositions from elastic-wave velocities obtained from seismic tomography. Some studies[12,14,18] suggest that temperature is the main factor which influences the seismic velocities at the depth of 50－250 km. So we can directly estimate the temperature structure of the lithospheric upper mantle from a 3D tomographic seismic velocity model. By this method, we obtained the upper-mantle temperature structure of the Chinese continent, from which we estimated the lithospheric thicknesses[10]. Here we will introduce the detailed upper-mantle temperatures, and the crustal temperatures constrained by the temperatures at the surface and upper mantle.

2 Method and data

2.1 Conversion of upper-mantle temperature from seismic velocity

In the seismic-thermal method proposed by Goes et al.[14], the elastic parameters and density are expressed as functions of temperature and pressure. After corrections for the anelasticity effect under high temperature, the elastic-wave velocities for a given condition of mineralogical composition, temperature and pressure can be calculated. For a given temperature (T), pressure (P), iron content (X_{Fe}) and under infinitesimal strain condition, the elastic parameters for a mineral can be presented as[14,19]

$$M(P,T,X_{\text{Fe}}) = M(P_0,T_0,0) + (T-T_0)\frac{\partial M}{\partial T} + (P-P_0)\frac{\partial M}{\partial P} + X_{\text{Fe}}\frac{\partial M}{\partial X_{\text{Fe}}}, \tag{1}$$

where M denotes the elastic parameter K or μ. Density ρ can be derived from K or μ[19]. For a rock with several different minerals, the rock's average elastic parameter $<M>$ can be calculated from the VRH average[14]. The shear-wave velocity may then be calculated from

$$V_s(P,T) = \sqrt{\frac{\langle\mu\rangle}{\langle\rho\rangle}}. \tag{2}$$

At a high temperature, it is necessary to correct for the anelasticity effect[14]. When anelasticity influence is weakly dependent on frequency (ω), the corrected velocity can be presented as[20]

$$V_s(P,T,\omega) = V_s(P,T)\left[1-\frac{Q^{-1}(\omega,T)}{2\tan(\pi a/2)}\right], \tag{3}$$

where Q is quality factor, the others are constant. The corrected velocity in eq. (3) is the expected shear-wave velocity under deep T and P condition. Here we use the anelasticicty model Q_1 of Goes et al.[14].

Studies[12,14,18,21] showed that temperature is the main factor influencing seismic velocities at the depth of

50－250 km. Goes et al.[14] showed that the composition variation of a rock can cause relatively small variation on seismic velocity (~1%) which normally lies in the uncertainty range of tomography. Therefore, we can directly invert for upper mantle temperatures from seismic velocities[15]. Since seismic tomography can offer fine-resolution 3D seismic-velocity structure, we can directly invert for 3D upper-mantle temperature using the tomographic seismic-velocity model. Analysis[14] showed that there may be ~150℃ of uncertainties in the inversion procedure from velocities to temperatures. For detailed description on this method, it should be referred to Goes et al.[14]. Here we used a direct grid search method to invert velocities for temperatures.

The continental upper mantle composition for different tectonic domains can be classified into two categories[19]: the off-cratonic and the on-cratonic composition. Because strong Phanerozoic tectonic events occurred in the Chinese continent, most regions have a young tectonothermal age. Therefore, we use an off-cratonic composition[19,22]: 68% olivine, 18% orthopyroxene, 11% clinopyroxene, 3% garnet and iron content 0.1.

Fluid effect can decrease seismic velocities[14]. But there is no model about the deep fluid distribution in the crust or the upper mantle. Therefore we did not consider the effect of fluids here. If the fluid influence is ignored and interpreted as the effect of temperature, the inverted temperatures will be higher and should be considered as the upper bound.

We use a 3D S-wave velocity model of Huang et al.[23], hereinafter the model is referred to as CN03S. This model results from a fundamental-mode Rayleigh wave dispersion (periods in 10－184 s) tomography which used more than 4000 ray paths, and has a lateral resolution of 4°－6° between 20°N and 45°N[23]. Based on the 2D dispersion results, Huang et al.[23] inverted for a 3D S-wave velocity model (CN03S) of the Chinese continent. Because the S-velocities in CN03S at a depth of 250 km are laterally very similar beneath all the studied regions, the model has bad resolution at depths ⩾250 km. Thus, we only use the S-velocities in CN03S down to a depth of 240 km. In addition to considering that the maximal crustal thickness in the continent is ~70 km beneath the Qinghai-Tibet Plateau, we only use the S-wave velocities in a depth range of 70－240 km in the inversion for temperatures.

Using the inverted upper-mantle temperature model to be discussed here, we (An and Shi[10]) estimated the lithospheric thicknesses for the Chinese continent. In that paper, we gave a detailed explanation on the possible uncertainties existing in the velocity model CN03S, and on the uncertainties existing in the temperature model. For reader's convenience to understand the results, we give a short introduction here. Huang et al.[23] did not offer the uncertainties of the model CN03S, but upper-mantle S velocities from a surface-wave dispersion study may have an uncertainty of < 0.1 km/s. The velocity change of 0.1 km/s can cause a change of ~50－250℃ in the upper-mantle temperature. Besides, compared with the off-cratonic composition used here, on-cratonic composition can cause an increase of the inverted temperature by ~15－120℃. When using anelasticity model Q_2[14], the calculated temperature can be up to ~180℃ lower than when using the model Q_1. Here we give an uncertainty of 150℃, as in Goes et al.[14].

2.2 Calculation of temperatures down to 80 km depth

Because of the complex of crustal composition, we use seismic velocity to invert for an upper-mantle temperature but not for crustal temperature. Instead, we estimate the crustal temperatures by solving the steady-state thermal conduction equation with the boundary conditions of the surface temperatures and the upper-mantle temperatures estimated above from seismic velocities. The steady-state thermal conduction equation[24] can be written as

$$\nabla \cdot (k \nabla T) = -A, \tag{4}$$

where A and k are heat productivity and conductivity, respectively.

In a tomography study, the uncertainty of Moho depth can cause some uncertainties in velocities around the Moho discontinuity and lead to uncertainties in the upper-mantle temperatures inverted from velocities. As the crustal thickness beneath the Qinghai-Tibet Plateau is ~70 km, we use the temperatures at a depth of 80 km as the bottom temperature boundary condition to calculate the steady-state conductive temperatures down to 80 km depth. In the calculation, we adopted the global CRUST2.0[25] as the crust model including sediments, the upper, middle and lower crust. The heat productivities of sediments and the upper crust are taken from Wang[3]; for the middle crust, the heat productivities are set as 0.4 μWm^{-3}[3,26], which is the maximum value used by Artemieva and Mooney[1]; for the heat productivities of the lower crust and upper mantle, we again follow Artemieva and Mooney[1] by setting them as 0.1 and 0.01 μWm^{-3}, respectively. Considering that both temperature and pressure have an obvious influence on conductivities of the upper crust[27], the conductivities are estimated from a relation[3,24] of conductivity (Wm^{-1} K^{-1}) with depth (D, in km) and temperature (℃): $3.0\times(1+0.0015D)/(1+0.0015T)$. Finally, we use constant conductivities for the other layers: 2.5 $Wm^{-1}K^{-1}$[3] for sediments; 2.25 Wm^{-1} K^{-1} for the middle crust, which is the average of the values used by Artemieva and Mooney[1]; and 2.0 and 4.0 Wm^{-1} K^{-1} for the lower crust and upper mantle respectively, also from Artemieva and Mooney[1].

3 One-D vertical temperature profiles for typical regions

The one-D temperature profiles (Figure 1) for some typical tectonic regions are discussed in detail below.

3.1 North China craton

Although the North China craton is one of the old blocks in China, it has been affected severely during Phanerozoic tectonic events, which caused the lithosphere to weaken during Mesozoic and Cenozoic, and then to form a complex structural framework. According to crustal structure characteristics, the North China craton can be divided into three parts from west to east[31]: (1) the Ordos basin, a stable paleo-continental block, has simple crustal structure and complete basement; (2) central orogenic belt, including the Taihang Mountain, north Yinshan and Yanshan orogenic belt, has relatively simple crustal structure and low velocity in the middle and lower crust; (3) eastern rift basin has a complex crustal structure, including depressed and destroyed basement, low seismic velocities, and thin crustal thickness, and typical characteristics of a Cenozoic crust.

The North China craton has been a focus of much geoscientific research, and there is a large number of published geological and geophysical works. Many geothermal scientists[3,24,28,32−34] have studied the craton's thermal structure, but with the steady-state thermal conduction assumption. Based on systematic studies of the average heat productivities of different cratonic rocks and different formations in the North China craton, Chi and Yan[28] calculated the thermal structure of the craton lithosphere.

Figure 1(a) shows the temperatures beneath the North China (Huabei) craton (excluding the Ordos basin). At the depth of ~90 km, our model reaches the adiabatic temperature of 1300℃, which may indicate that the lithosphere bottom is at ~90 km depth since this adiabatic temperature is normally defined as the temperature at the base of the thermal lithosphere. This result is consistent with the depth of the top of the seismic low velocity zone, also shown in Figure 1(a). Such consistency indicates that the upper-mantle low velocity zone may be related to the melting temperature of upper mantle rocks[10].

Figure 1(a) also shows the temperature model of Wang[3] which is calculated from measured surface heat flow with the steady-state thermal conduction assumption. The difference between the Wang's model and our result becomes significant at depths below the Moho. At a depth of 70 km, the temperature in Wang's model is ~150℃ greater than that in our model, which is nearly equal to the uncertainty in the conversion procedure from seismic-velocities to temperatures.

3.2 Ordos basin

The Ordos basin shows different characteristics from the other parts of the North China craton. In contrast with the other parts of the craton, the Ordos basin has a simple crustal structure with a complete basement and a stable paleo-continental crust[31]. As the average heat flow of the North China craton from the work of Chi and Yan[28] is consistent with the heat flow of the Ordos basin used by Wang[3], we plotted the temperature profile of the North China craton of Chi and Yan[28] together with the present temperature profile of the Ordos basin in Figure 1(b).

In the temperature profiles for the Ordos basin (Figure 1(b)), both the results of Chi and Yan[28] (dots) and of Wang[3] are based on steady-state thermal conduction and constrained by surface heat flow observations. Although the thermal parameters used in these two works are slightly different, Figure 1(b) shows that the results in the two works are basically similar. In contrast, our temperature model above 80 km deep is higher, and the difference mainly exists in the upper mantle (Figure 1(b)). At a depth of 70 km, our temperature is ~150℃ greater than Wang's.

Figure 1(b) shows that the temperature beneath the

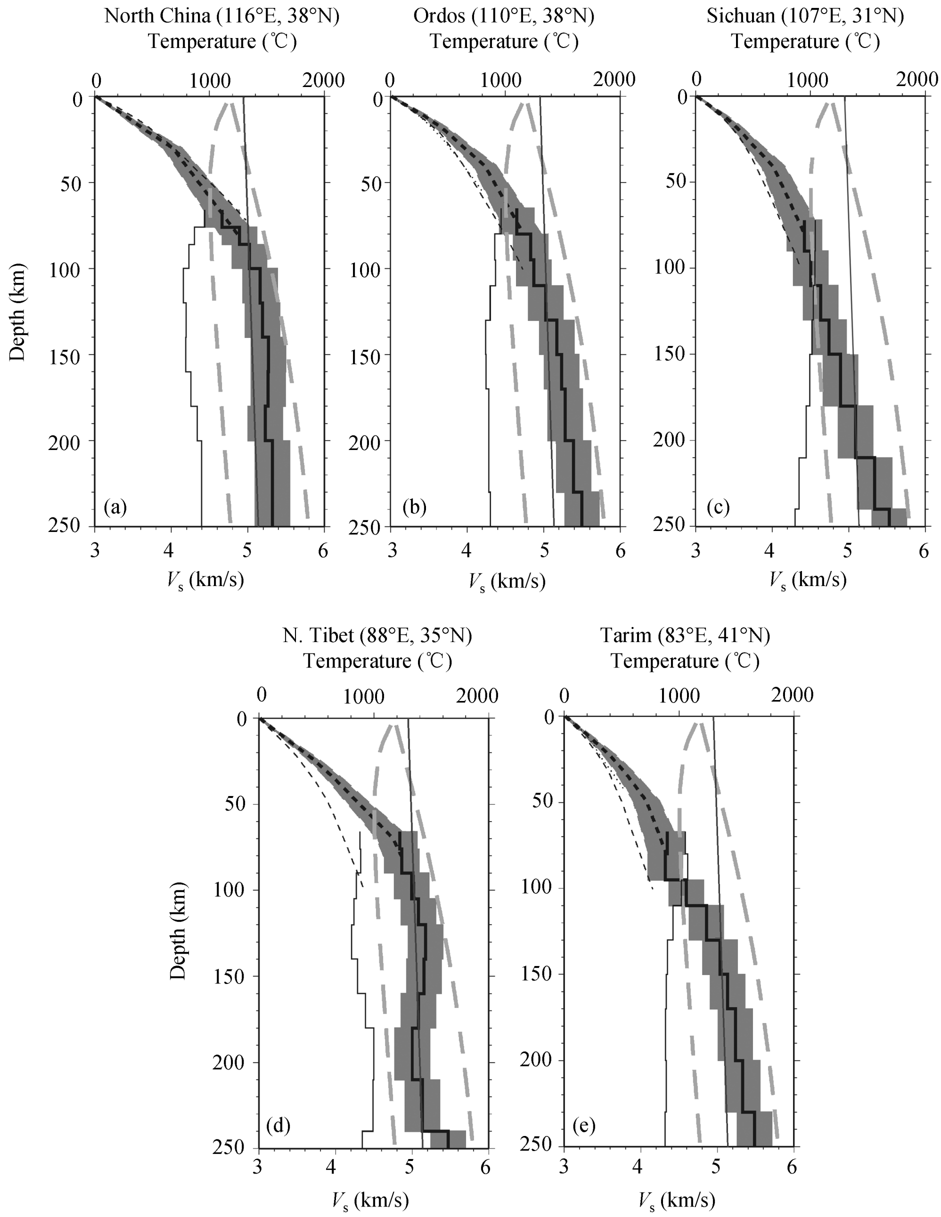

Figure 1 One-dimensional temperature and seismic velocity profiles for several typical regions in the Chinese continent. The locations of the profiles are shown in Figure 2. Thick line represents upper mantle temperatures calculated from seismic velocities (thin black line) and gray shaded area is the temperature uncertainty range of ±150℃. Because the heat productivity of the upper mantle is very small, the temperature profiles show a change in slope at the depth of the Moho. Thick dashes are the steady-state thermal conduction temperatures calculated with the constraints of the Earth's surface temperature and the temperature at the depth of 80 km. Dots and thin dashes are the temperatures estimated from observed surface heat flow using the steady-state assumption. The thin dashes are temperatures from Wang[3], the dots for the Ordos basin are temperatures from Chi & Yan[28] and those for the Tarim craton are temperatures from Liu et al.[29]. Grey dashes are the melting temperatures of wet (with water) and dry peridotites[30]. Grey line is the 1300℃ adiabat. The lable "North China" means the North China craton, "Ordos" the Ordos basin, "Sichuan" the Sichuan basin, "Tarim" the Tarim craton.

Ordos basin reaches the adiabatic temperature of 1300℃ at a depth of ~110 km, which indicates that the lithosphere is thicker than that of the other parts in the North China craton.

3.3 Sichuan basin

After its development period from Sinian to Middle Triassic, the Yangtze craton has been affected by the Pacific Ocean plate and the Tethyan plate since Late Triassic. Tectonic events partially reshaped the old tectonic framework. The Sichuan basin is the most stable block in the Yangtze craton.

Figure 1(c) shows that Wang's temperatures[3] for the Sichuan basin are lower than our results in the depth of

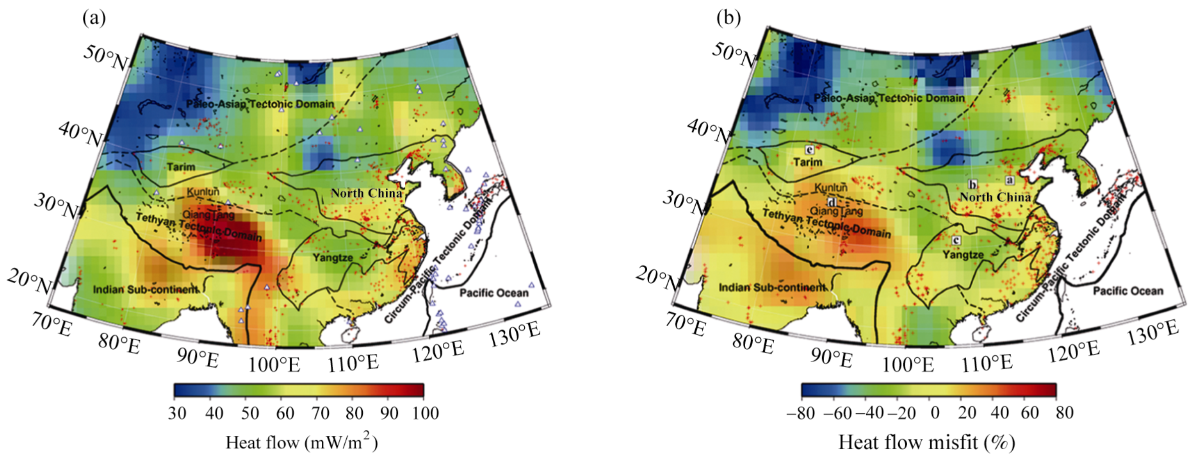

Figure 2 Surface heat flow (a) and the misfit (b) between observed and the calculated surface heat flow, i.e., (observed – calculated)/observed. The observed heat flow in (a) was obtained by a Kriging interpolation between heat flow measurements at locations marked by the cross symbols. Open triangles are volcanoes, data from Smithsonian Institution, Global Volcanism Program. The squares in (b) represent locations of the profiles in Figure 1. The label "Tarim" means the Tarim craton, "Kunlun" the Kunlun Mountains, "Qiang Tang" the Qiangtang terrane, "North China" the North China craton, and "Yangtze" the Yangtze craton.

40—100 km, e.g., at 70 km depth the difference is ~150℃. The present temperature model beneath the Sichuan basin reaches the adiabatic temperature of 1300℃ at a depth of ~180 km.

3.4 Qiangtang terrane

In a seismic waveform study, Rodgers and Schwartz[35] found a low velocity zone in the lithospheric upper mantle beneath the Qiangtang terrane of northern Tibet. They proposed that the low velocity may represent upper mantle partial melting or a back arc upper mantle produced by the early Tethyan subduction. The presence of this low velocity layer is also supported by later surface wave studies (e.g., Huang et al.[23] and Su et al.[36]) and body-wave studies. The body-wave results support the partial melting hypothesis, e.g., Sn wave could not propagate in the Qiangtang area[37] and Pn-wave velocity is low[38]. An and Shi[10] showed that the temperature of this low velocity zone exceeded the adiabat of mantle potential temperature. The temperature profile in Figure 1(d) shows that the seismic-thermal temperature for the northern Tibet is higher than the adiabatic temperature of 1300℃ at the depth of 110—150 km, while below 160 km depth the temperature is lower than the adiabatic temperature. So the high temperature at 110—150 km depth is only a local anomaly. As mentioned previously, we did not consider fluid influence in the conversion from velocities to temperatures; thus the calculated temperature at 110—150 km depth should be upper bound.

In deep part, the model of Wang[3] is ~400℃ lower than our estimated temperatures up to 80 km depth (Figure 1(d)). Observations show that the heat flow of northern Tibet is ~45 mWm^{-2}, which is similar to the heat flow of the Tarim craton on its west and lower than that of southern Tibet and the Qaidam basin on its north. Considering the low seismic velocity[23,36] and high temperature at the depth of 110—115 km in Figure 1(d), we suggest that the crust of northern Tibet is colder than that of southern Tibet and the Qaidam basin, but the upper mantle is hotter. A possible interpretation of this temperature profile is that the upper mantle was heated up by some geological processes, but this heat has not yet reached the surface by thermal conduction; thus the lithosphere is not in a thermal steady state.

3.5 Tarim craton

Since the collision between the Indian and Eurasian continents starting at the end of Eocene, the continuous compression between the two plates caused intraplate contraction, detachment and decoupling of the subduction slab. The weak deformation in the Tarim craton implied that the detachment and decoupling had not/less occurred[39]. The group of Wang[29,40] successively studied the thermal structures of the Tarim craton.

Figure 1(e) shows that the model of Wang[3] is lower than our results in the Tarim craton by ~150℃ at a depth of 40 km and ~260℃ at 70 km. The model from Liu et al.[29] shows a smaller difference (~100℃ at 40 km depth) from our results. The crossing position with the 1300℃ adiabat by extrapolating from Wang's temperatures occurs at ~235 km depth, which is quite different from our result of ~150 km.

The Tarim craton and Qiangtang basin are relatively less surveyed with seismic methods, while the other three blocks were all covered by deep seismic sounding[41]. By comparing the temperature profiles of the North China craton, the Ordos and Sichuan basins, it appears that the 1300℃ adiabat was crossed by the previous studies based on heat flow constraints at similar depth to by our results based on the seismic-thermal conversion. Since the seismic-thermal results derived from velocities are consistent with seismological results, the previous studies are also consistent with the seismic low-velocity zone in these regions. Except for the above-mentioned three regions, however, the position crossing the 1300℃ adiabat in the previous studies of the Tarim craton is quite different from our present results and the top of the seismic low velocity zone. In view of the dynamic processes related to the Indian-Eurasian continental collision, the deep thermal structures beneath the Qiangtang terrane and the Tarim craton are likely to be very complex; the uncertainties in the temperatures derived from surface heat flow and the steady-state assumption are likely to be relatively high.

4 Temperatures at several depths

Figure 3 shows the crustal temperatures at 25 km depth, and Figures 4—6 are the upper mantle temperatures at 100 km, 150 km and 200 km, respectively.

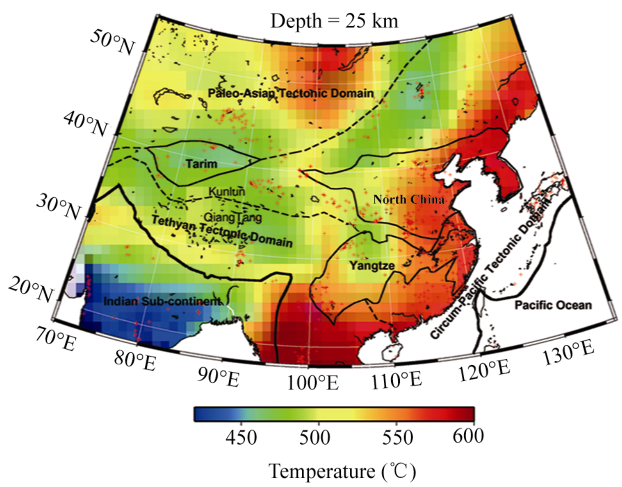

Figure 3 Crustal temperatures at a depth of 25 km. The others are the same as in Figure 2.

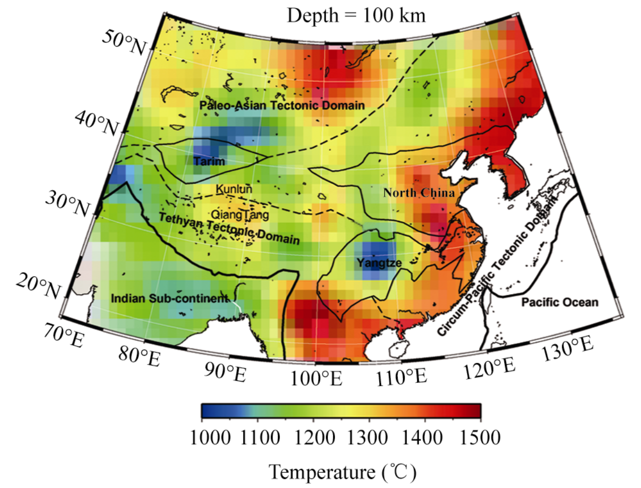

Figure 4 Upper-mantle temperatures at 100 km depth. The adiabatic temperature of 1300℃ at the depth of 100 km is ~1361℃. The others are the same as in Figure 2.

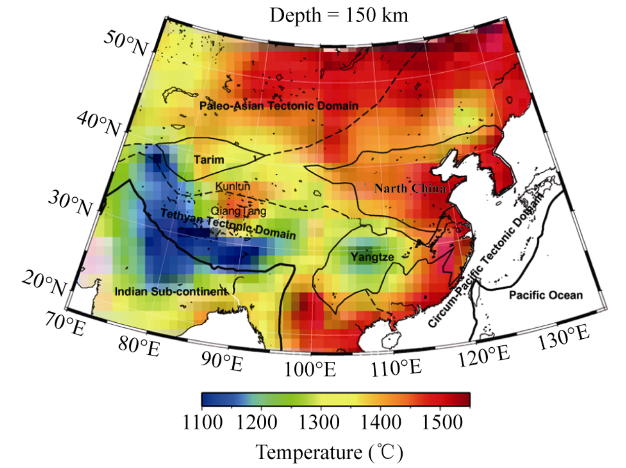

Figure 5 Upper-mantle temperatures at 150 km depth. The 1300℃ adiabatic temperature at the depth of 150 km is ~1392℃. The others are the same as in Figure 2.

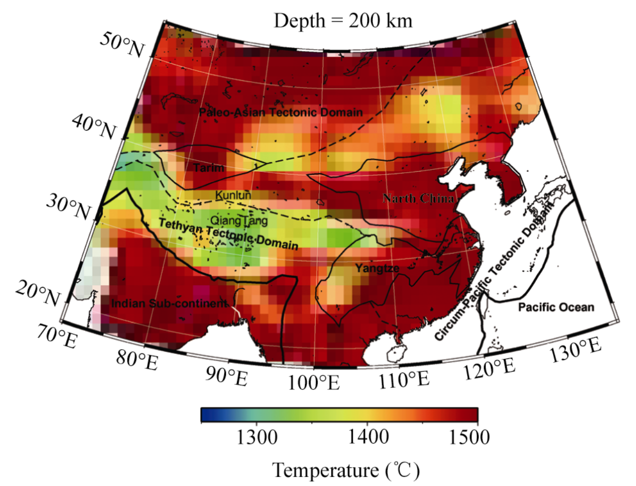

Figure 6 Upper-mantle temperatures at 200 km depth. The 1300℃ adiabatic temperature at the depth of 200 km is ~1424℃. The others are the same as in Figure 2.

4.1 Crustal temperature

The crustal temperatures are obtained from the steady-state thermal conduction assumption with the boundary conditions of the temperatures at the Earth's surface and at the depth of 80 km. We do not use surface heat flow as a constraint. Instead, we calculate the surface heat flow from our calculated temperatures and compare these with the observed heat flow (Figure 2(b)). The observed surface heat flow data for China and Asia are collected from a global database (http://www.heatflow.und.edu/index2.html); the detailed description on the data for China can be found in relevant works[42−44]. Figure 2(b) shows that the misfit of the calculated and observed heat flow for most regions of China lies inside of ±20%, especially for regions with dense measurements such as the Tarim craton, eastern and western Yangtze craton, South China, southern and western North China craton. However, some regions with fewer measurements have high misfit, such as in northwestern North China craton, the misfit can be as high as −40% (Figure 2(b)); in Tibet, the observed heat flow is much higher than our calculated values. The distribution of heat flow measurements in Tibet is extremely uneven. Most of the measurements located around the position (N30°, E90°) and two isolated measurements at Lunpola and Naqu give very high heat flow values (Table 1).

For regions without measurement, we interpolated the heat flow values of the surrounding regions by a Kriging interpolation, and the interpolated values (Figure 2(a)) are taken as the observed heat flow. The interpolated values in Tibet from the two isolated high-heat-flow measurements may also be higher than the actual average heat flow of the area. Thus the high difference (~40%) between the observed and calculated heat flow (Figure 2(b)) may indicate that the few measured heat flow is not representative of the region. Table 1 also shows that most of the measurements are in low quality and those with values higher than 100 mWm^{-2} are ranked 'D' in quality which indicates that the data do not represent the regional thermal state. Hence the large difference between the calculated and observed heat flow in Tibet does not constitute a negative test of the present model.

In sum, the misfit of the calculated and observed heat flow lies within the observation errors for most regions where dense and high-quality measurements are available. Therefore, our calculated crustal thermal structure may represent the general crustal thermal state. Comparisons with the 1D temperature profiles, discussed in the last section, also show that the results are internally consistent.

At 25 km depth, the crust shows higher temperatures in the east and lower temperatures in the west (Figure 3).

Table 1 Observed heat flow data in Tibet (from Wang & Huang[44])

No.	Location	Latitude (°N)	Longtitude (°E)	Heat flow (mWm^{-2})	Quality
1	Lunpola	32.019167	89.741667	140	B
2	Yangyingxiang	28.566667	90.445833	87.9	D
3	Pumoyong Lake	30.11	90.47	95.5	A
4	Pumoyong Lake	28.5625	90.475	87.9	A
5	Yangbajing	28.579167	90.470833	87.9	B
6	Pumoyong Lake	28.558333	90.406667	90	A
7	Pumoyong Lake	28.566667	90.479167	100.1	A
8	Pumoyong Lake	28.845833	90.6125	152	A
9	Yamzho Yumco Lake	28.858333	90.625	242	D
10	Yamzho Yumco Lake	29.170833	90.616667	126.9	D
11	Yamzho Yumco Lake	30.253333	90.645	267	D
12	Laduogang	29.133333	90.691667	165.8	D
13	Yamzho Yumco Lake	29.828333	90.316667	271	D
14	Yamzho Yumco Lake	28.979167	90.75	138.2	D
15	Maqu	29.906667	90.813333	106	B
16	Lhasa	29.675	90.098333	66	B
17	Naqu	31.498333	92.05	319	D
18	Luobusha	29.25	91.98333	61	A

Quality D means that the measurement cannot represent regional and deep thermal state.

The temperatures are ~500－600℃ in the east and less than 500℃ in the west. In the Tarim craton, the temperatures are the lowest, reaching ~460℃. As the crustal structure in western China is more complex than in eastern China, the crustal temperature in west China has less reliability than in eastern China.

4.2 Upper-mantle temperature

At a depth of 100 km, the upper-mantle temperatures of the Chinese continent are higher in the east than in the west (Figure 4). The temperatures in the east and southeast China (including eastern NE China, eastern North China craton, eastern Yangtze craton and South China) are generally higher than the adiabatic temperature of 1300℃. Thus the lithosphere beneath these regions may be thinner than 100 km. On the other hand, the temperatures in the west are from 1100 to 1300℃. Hence the lithosphere beneath western China may be thicker than 100 km. The two oldest cratons (the Tarim craton and the Sichuan basin of the Yangtze craton) show a low temperature (~1000℃) at this depth.

The temperature distribution at 150 km depth is more complex (Figure 5). At this depth, the temperatures beneath the entire North China craton, besides in South China and eastern Yangtze craton, are greater than the adiabatic temperature of 1300℃. The temperatures beneath the Qiangtang terrane also reach the adiabatic temperature. The Sichuan basin shows a low temperature at this depth, while the central Tarim craton shows higher temperature than its surrounding area. The lowest temperature (~1130℃) is found in the regions close to the collision zone of the Indian subcontinent and the Chinese continent (e.g. Himalayas).

The temperature distribution at 200 km depth shows a good relationship with the regions strongly affected by the collision and subduction from the Indian subcontinent (Figure 6). Temperatures beneath the north to the collision zone (e.g., the Qinghai-Tibet Plateau, Kunlun Mountains to the south of the Tarim craton) are lower temperature than the adiabatic temperature of 1300℃ at this depth. Since the Qinghai-Tibet Plateau has lower temperatures than the adiabatic temperatures of 1300℃ at almost all depths as discussed above, the thickness of its lithosphere may be greater than 200 km. On the other hand, the two oldest cratons do not show any more low temperature anomaly at this depth.

5 Discussions

In the following discussion we clarify the methodology and concepts used in the present study and differences with the previous steady-state thermal conduction studies.

5.1 The relation between seismic velocity and upper mantle temperature

From the conversion from seismic velocities to temperatures on the basis of a homogeneous off-cratonic composition, the resultant upper-mantle temperatures cross the 1300℃ adiabat at a depth which is about the top of the seismic low velocity zone[10]. This depth consistency may imply that our estimated temperatures are reliable and can represent the thermal structure of the upper mantle. Moreover, this consistency also implies that the seismological lithosphere based on seismic velocities may be compatible or consistent with the thermal lithosphere defined by temperatures.

5.2 Function of observed heat flow

Because we take the upper-mantle and surface temperatures as the boundary conditions in the calculation of the steady-state temperature distribution, this calculation is like a temperature interpolation but not extrapolation mainly constrained by the surface heat flow as done by the previous traditional studies. The surface heat flow data are instead to test the calculated heat flow as an appraisal of the calculated temperature model.

5.3 Function of seismic velocity

In the previous geothermal studies, seismic velocities are used as a reference in estimating thermal conductivity and heat productivity, while in the present study seismic velocities are used to estimate the deep temperatures.

5.4 Steady-state and transient temperature

The major difficulty in the previous studies is lack of good deep thermal constraint, so the estimated temperature strongly depends on the steady-state thermal conduction assumption which implicitly assumes that the lithosphere was stable for a long period. As discussed earlier, the errors arising from this assumption increases with depth and the result will be highly uncertain in area with complex deep structures where the assumption of long-time stability is extremely uncertain.

The tomographic seismic velocity shows the present (transient in geological time) state, so the upper mantle temperatures derived from seismic velocities represent the present.

In the calculation of the temperatures down to 80 km depth, since we used the temperatures at the surface and at a depth of 80 km as the boundary conditions and solved the steady-state conduction equation, our calculated temperatures may represent a first-order approximation down to 80 km depth.

6 Conclusions

In the present study we derived the 3D upper-mantle thermal structure for the Chinese continent using S-wave velocities, and then estimated the thermal structure down to 80 km by solving the steady-state conduction equation with the boundary conditions of the temperatures at the surface and at 80 km depth. The difference between the calculated and observed surface heat flow is less than 20% which is within the observational error of the heat flow measurement.

At a depth of 25 km, higher temperatures (~500—600℃) occur in the east and lower temperatures (< 500℃) occur in the west; the Tarim craton has the lowest temperature (~460℃).

At a depth of 100 km, the temperatures in the east are also higher and lower in the west. Beneath most of eastern and northeastern China (including eastern NE China, eastern North China craton, eastern Yangtze craton and South China), temperatures are higher than the adiabatic temperature of 1300℃ at this depth, while it is between 1100 and 1300℃ beneath most of western China. Beneath the two old stable cratons, the Tarim craton and Sichuan basin, temperatures are ~1000℃.

At a depth of 150 km, beneath the entire North China craton, besides South China and eastern Yangtze craton, temperatures are higher than the adiabatic temperature of 1300℃; it also reaches the adiabatic temperature beneath the Qiangtang terrane. For the two old stable cratons, the Sichuan basin shows a low temperature of ~1150℃, but the center of the Tarim craton shows higher temperatures than its surrounding area. The temperatures beneath the collision zone between the Indian subcontinent and the Chinese continent are the lowest (~1100℃).

The temperatures at 200 km depth show a good relation with the regions strongly affected by the Indian subcontinent collision. North of the collision zone, including the Qinghai-Tibet Plateau and Kunlun Mountains to the south of Tarim, temperatures are lower than 1300℃. The two old stable cratons, on the other hand, did not show low temperature anomaly at this depth.

Thanks to Prof. Huang Zhongxian for kindly offering the 3D S-wave velocity model. Cao Jianling gave a help in the calculation of steady-state thermal conduction. Thanks to Dr. S. Goes and N. M. Shapiro gave suggestion to improve the seismic-thermal calculation, and for the reviewers' constructive comments. Thanks to Prof. Chi-Yuen Wang for kindly helping to improve the manuscript.

1 Artemieva I M, Mooney W D. Thermal thickness and evolution of Precambrian lithosphere: A global study. J Geophys Res, 2001, 106(B8): 16387—16414
2 Hu S P, Wang J Y, Wang Y H. Deep temperature and lithospheric thickness along the eastern segment of the Heishui-Quanzhou geotraverse. Acta Geophys Sinica (in Chinese), 1994, 37(3): 330—337
3 Wang Y. Heat flow pattern and lateral variations of lithosphere strength in China mainland: constraints on active deformation. Phys Earth Planet In, 2001, 126: 121—146
4 Wang Y, Wang J Y, Xiong L P, et al. Lithospheric geothermics of major geotectonic units in China mainland. Acta Geosci Sinica (in Chinese), 2001, 22(1): 17—22
5 Huang S B, Wang J Y, Chen M X. Temperature at the Moho. In: Yuan X, ed. Atlas of Geophysics in China (in Chinese). Beijing: Geological Publishing House, 1996. 105—107
6 Powell W G, Chapman D S, Balling N, et al. Continental heat flow density. In: Haenel R, Rybach L, Stegens L, eds. Handbook of Terrestrial Heat-Flow Density Determination. Dordrecht: Kluwer Academic Publishers, 1988. 167—222
7 Mareschal J C, Jaupart C. Variations of surface heat flow and lithospheric thermal structure beneath the North American craton. Earth Planet Sci Lett, 2004, 223: 65—77
8 Ren J S, Wang Z X, Chen B W, et al. The Tectonics of China From a Global View —A Guide to the Tectonic Map of China and Adjacent Regions (in Chinese). Beijing: Geological Publishing House, 1999. 1—32
9 Jaupart C, Mareschal J C. The thermal structure and thickness of continental roots. Lithos, 1999, 48: 93—114
10 An M, Shi Y. Lithospheric thickness of the Chinese continent. Phys Earth Planet In, 2006, 159: 257—266
11 Zhang Y S, Tanimoto T. High-resolution global upper mantle structure and plate tectonics. J Geophys Res, 1993, 98: 9793—9823
12 Sobolev S V, Zeyen H, Stoll G, et al. Upper mantle temperatures from teleseismic tomography of French Massif Central including effects of composition, mineral reactions, anharmonicity, anelasticity and partial melt. Earth Planet Sci Lett, 1996, 139(1-2): 147—163
13 Sobolev S V, Zeyen H, Granet M, et al. Upper mantle temperatures and lithosphere-asthenosphere system beneath the French Massif Central constrained by seismic, gravity, petrologic and thermal ob-

servations. Tectonophysics, 1997, 275(1-3): 143－164
14 Goes S, Govers R, Vacher P. Shallow mantle temperatures under Europe from P and S wave tomography. J Geophys Res, 2000, 105(B5): 11153－11169
15 Goes S, Van der Lee S. Thermal structure of the North American uppermost mantle inferred from seismic tomography. J Geophys Res, 2002, 107(B3): 2050
16 Cammarano F, Goes S, Vacher P, et al. Inferring upper-mantle temperatures from seismic velocities. Phys Earth Planet In, 2003, 138(3-4): 197－222
17 Röhm A H E, Snieder R, Goes S, et al. Thermal structure of continental upper mantle inferred from S-wave velocity and surface heat flow. Earth Planet Sci Lett, 2000, 181: 395－407
18 Nolet G, Zielhuis A. Low S velocities under the Tornquist-Teisseyre zone: evidence for water injection into the transition zone by subduction. J Geophys Res, 1994, 99: 15813－15820
19 Shapiro N M, Ritzwoller M H. Thermodynamic constraints on seismic inversions. Geophys J Int, 2004, 157: 1175－1188
20 Minster J B, Anderson D L. A model of dislocation-controlled rheology for the mantle. Phil Trans R Soc Lond A, 1981, 299: 319－356
21 Jordan T H. Mineralogies, densities and seismic velocities of garnet lherzolites and their geophysical implications. In: Boyd F R, Myer H O A, eds. The Mantle Sample: Inclusions in Kimberlites and Other Volcanics. AGU, Washington, D.C., 1979. 1－14
22 McDonough W F, Rudnick R L. Mineralogy and composition of the upper mantle. In: Hemley R J, ed. Ultrahigh-pressure Mineralogy: Physics and Chemistry of the Earth’s Deep Interior. Washington, DC: Mineralogical Society of America, 1998. 139－164
23 Huang Z, Su W, Peng Y, et al. Rayleigh wave tomography of China and adjacent regions. J Geophys Res, 2003, 108(B2): 2073
24 Zang S X, Liu Y G, Ning J Y. Thermal structure of the lithosphere in north China. Chinese J Geophys, 2002, 45(1): 51－62
25 Bassin C, Laske G, Masters G. The current limits of resolution for surface wave tomography in North America. EOS Trans AGU, 2000, 81: F897
26 Pinet C, Jaupart C. The vertical distribution of radiogenic heat production in the Precambrian crust of Norway and Sweden: geothermal implications. Geophys Res Lett, 1987, 14: 260－263
27 Chapman D S, ed. Thermal gradients in the continental crust. Geological Society Special Publication, 1986. 63－70
28 Chi Q H, Yan M C. Radioactive elements of rocks in North China platform and the thermal structure and temperature distribution of the modern continental lithosphere. Acta Geophys Sinica (in Chinese), 1998, 41(1): 38－48
29 Liu S W, Wang L S, Li C, et al. Thermal-rheological structure of lithosphere beneath the northern flank of Tarim Basin, western China: Implications for geodynamics. Sci China Ser D-Earth Sci, 2004, 47(7): 659－672
30 Thompson A B. Water in the Earth's upper mantle. Nature, 1992, 358: 295－302
31 Jia S X, Zhang X K. Crustal structure and comparison of different tectonic blocks in North China. Chin J Geophys, 2005, 48(3): 672－683
32 Wang J Y. Geothermics in China. Beijing: Seismological Press, 1996. 1－300
33 Chen M X, ed. Geothermics of North China (in Chinese). Beijing: Science Press, 1988. 1－218
34 Yang S Z, Lu X W. Study on thermal conductive structure of the upper part of the crust in North China. Acta Petrol Sinica (in Chinese), 1985, 1(2): 64－73
35 Rodgers A J, Schwartz S Y. Lithospheric structure of the Qiangtang Terrane, northern Tibetan Plateau, from complete regional waveform modeling: Evidence for partial melt. J Geophys Res, 1998, 103(B4): 7137－7152
36 Su W, Peng Y J, Zheng Y J, et al. Crust and upper mantle shear velocity structure beneath the Tibetan Plateau and adjacent areas. Acta Geosci Sinica (in Chinese), 2002, 23(3): 193－200
37 Ni J, Barazangi M. Velocities and propagation characteristics of Pn, Pg, Sn, and Lg seismic waves beneath the Indian Shield, Himalayan Arc, Tibetan Plateau, and surrounding regions: High uppermost mantle velocities and efficient Sn propagation beneath Tibet. Geophys J R Astr Soc, 1983, 72: 665－689
38 McNamara D E, Walter W R, Owens T J, et al. Upper mantle velocity structure beneath the Tibetan Plateau from Pn travel time tomography. J Geophys Res, 1997, 102(B1): 493－506
39 Li T, Wang Z X. The lithospheric decoupling of the Tarim Basin and surrounding orogenic belts and its relationship with basin-mountain patterns from the analysis of natural earthquake. Earth Sci Front (In Chinese), 2005, 12(3): 125－136
40 Wang L S, Li C, Yang C. The Lithospheric thermal structure beneath Tarim basin, western China. Acta Geophys Sinica (in Chinese), 1996, 39(6): 795－803
41 Teng J W. Great achievements in geophysics in the 20th century and developing frontiers for the 21st century. Earth Sci Front (in Chinese), 2003, 10(1): 117－140
42 Hu S, He L, Wang J. Heat flow in the continental area of China: a new data set. Earth Planet Sci Lett, 2000, 179(2): 407－419
43 Hu S B, He L J, Wang J Y. Compilation of heat flow data in the China continental area (3rd ed.). Chin J Geophys, 2001, 44(5): 604－618
44 Wang J Y, Huang S P. Compilation of heat flow data in the China continental area (2nd ed.). Seismol Geol (in Chinese), 1990, 12(4): 351－366